



Since January 2020 Elsevier has created a COVID-19 resource centre with free information in English and Mandarin on the novel coronavirus COVID-19. The COVID-19 resource centre is hosted on Elsevier Connect, the company's public news and information website.

Elsevier hereby grants permission to make all its COVID-19-related research that is available on the COVID-19 resource centre - including this research content - immediately available in PubMed Central and other publicly funded repositories, such as the WHO COVID database with rights for unrestricted research re-use and analyses in any form or by any means with acknowledgement of the original source. These permissions are granted for free by Elsevier for as long as the COVID-19 resource centre remains active.



Repurposing of anti-lung cancer drugs as multi-target inhibitors of SARS-CoV-2 proteins: An insight from molecular docking and MD-simulation study

Rahimasoom Reza^a, Tanmoy Dutta^b, Nabajyoti Baildya^c, Narendra Nath Ghosh^d, Abdul Ashik Khan^e, Rajesh Kumar Das^{a,*}

^a Department of Chemistry, University of North Bengal, Darjeeling, 734013, India

^b Department of Chemistry, JIS College of Engineering, Kalyani, 741235, India

^c Department of Chemistry, University of Kalyani, Kalyani, 741235, India

^d Department of Chemistry, University of Gour Banga, Mokdumpur, Malda, 732103, India

^e Department of Chemistry, Darjeeling Government College, Darjeeling, 734101, India

ARTICLE INFO

Keywords:

SARS-CoV-2

Capmatinib

Molecular dynamics simulation

Mpro

PLpro

Spike protein

ABSTRACT

Herein we have selected seventeen anti-lung cancer drugs to screen against Mpro, PLpro and spike glycoproteins of SARS-CoV-2 to ascertain the potential therapeutic agent against COVID-19. ADMET profiling were employed to evaluate their pharmacokinetic properties. Molecular docking studies revealed that Capmatinib (CAP) showed highest binding affinity against the selected proteins of SARS-CoV-2. Molecular Dynamics (MD) simulation and the analysis of RMSD, RMSF, and binding energy confirmed the abrupt conformational changes of the proteins due to the presence of this drug. These findings provide an opportunity for doing advanced experimental research to evaluate the potential drug to combat COVID-19.

1. Introduction

World health and economy were greatly affected by the pandemics of COVID-19 [1,2]. Virus genome sequence [3] of SARS-CoV-2 was genetically related to the coronavirus, responsible for the outbreak in 2003 [4,5]. The etiologic agent of COVID-19 was isolated and identified as a noble coronavirus, initially designated as 2019-nCoV [6]. Symptoms may vary among persons that includes brain or lungs failure also in some major cases [7,8]. SARS-CoV-2 belongs to the corona viridae family, an enveloped single-stranded positive sense RNA virus [9,10]. The main protease (Mpro), also known as 3-C like protease(3CLpro), has a crucial role in posttranslational processing of the replicase polyproteins [11]. Papain-like protease (PLpro) has the ability to disrupt the viral sequence and enhances viral load in host cell [12]. Spike protein, a transmembrane structural protein has two subunit S1 and S2; S1 with RBD region is responsible for the binding to the host cell whereas S2 for the viral cell membrane fusion [13,14]. Still now there are no appropriate drugs which inhibit the functions of different proteins like Mpro, PLpro and Spike protein restoring innate immune responses of host.

The best strategy to develop an efficient drug against COVID-19 is repurposing of the available active drugs in the market [15]. Only few drugs like, Remdesivir [16], Chloroquine [17], hydroxychloroquine [18,19], Favipiravir [20], Triazavirin [21] showed a ray of hope but none of these are efficient at the satisfactory level [22]. An extensive study showed that few RNA virus drugs showed inhibitory efficacy against COVID-19 [23]. Again, few plants extract showed potency against SARS-Cov-2 [24–26].

In the present study 24 anti-lung cancer drugs have been selected out of which 17 drugs follow Lipinski's rule [27]. Binding energy of all 17 drugs is calculated with the viral proteins like Mpro, PLpro, and spike protein. The binding efficiency value of 8 selected drugs are equal or more than frequently used SARS-CoV-2 drugs such as Remdesivir, Chloroquine, Hydroxychloroquine, Favipiravir, Triazavirin [28]. Furthermore, we have checked Absorption, Distribution, Metabolism, Excretion and Toxicity(ADMET) [29] profile of these anti-lung cancer drugs. The binding stability of the viral proteins (Mpro, PLpro, Spike) with the drug Capmatinib (CAP) are established by the analysis of different parameters like RMSD, RMSF, SASA and GYRATE with the help

* Corresponding author.

E-mail addresses: rahimasoom888@gmail.com (R. Reza), dutta.tanmoy88@gmail.com (T. Dutta), nabajyotibaildya@gmail.com (N. Baildya), ghosh.naren13@gmail.com (N.N. Ghosh), abdulashik0@gmail.com (A.A. Khan), rajeshnbu@gmail.com (R.K. Das).

<https://doi.org/10.1016/j.micpath.2022.105615>

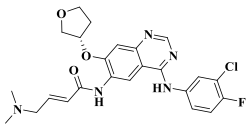
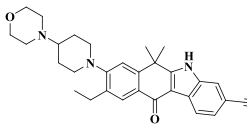
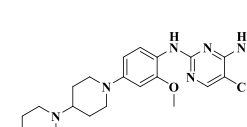
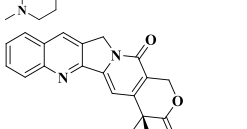
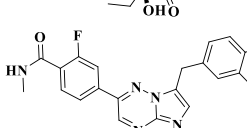
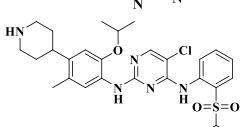
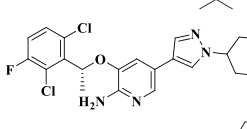
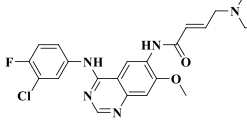
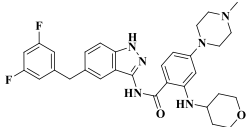
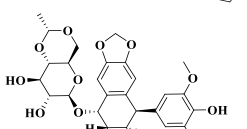
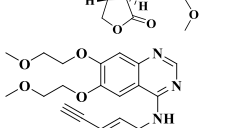
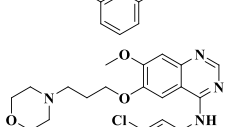
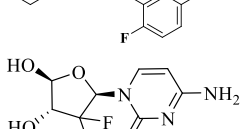
Received 4 October 2021; Received in revised form 2 June 2022; Accepted 2 June 2022

Available online 8 June 2022

0882-4010/© 2022 Elsevier Ltd. All rights reserved.

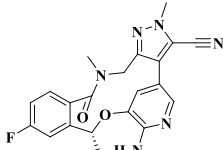
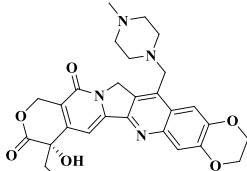
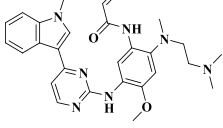
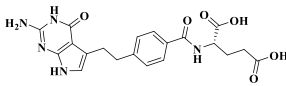
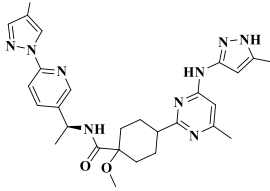
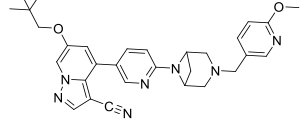
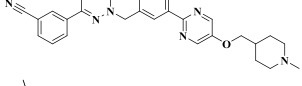
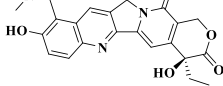
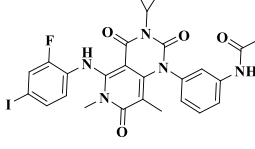
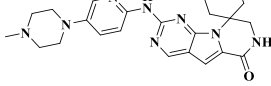
Table 1

List of the anti-lung cancer drugs with their structure, molecular weight, partition coefficient (log P) and number of hydrogen bond donor-acceptor sites.

Drug Name	Structure	Molecular Weight (MW)	logP	H-bond donor	H-bond acceptor	Follow Lipinski's rule
Afatinib [39]		485.9	4.3899	2	7	Yes
Alectinib [40]		482.6	4.7730	1	5	Yes
Brigatinib [41]		584.105	5.0900	2	9	No
Camptothecin [42]		348.358	2.0800	1	6	Yes
Capmatinib [43]		412.428	3.4290	1	6	Yes
Ceritinib [44]		558.148	6.3620	3	8	No
Crizotinib [45]		450.345	5.0400	2	6	Yes
Dacomitinib [46]		469.948	5.1600	2	6	No
Entrectinib [47]		460.649	5.030	3	6	Yes
Etoposide [48]		488.562	1.3386	3	13	Yes
Erlotinib [49]		393.443	3.4051	1	7	Yes
Gefitinib [50]		446.91	4.2756	1	7	Yes
Gemcitabine [51]		263.2	-1.2886	3	7	Yes

(continued on next page)

Table 1 (continued)

Drug Name	Structure	Molecular Weight (MW)	logP	H-bond donor	H-bond acceptor	Follow Lipinski's rule
Lorlatinib [52]		406.421	2.8007	1	7	Yes
Lurtotecan [53]		518.57	1.5982	1	10	No
Mechlorethamine [54]	<chem>ClCCN(C)CCCl</chem>	156.05	1.8200	0	1	Yes
Osimertinib [55]		499.619	4.5100	2	8	Yes
Pemetrexed [56]		427.42	0.6664	6	6	Yes
Pralsetinib [57]		433.612	4.20014	3	9	Yes
Selpercatinib [58]		525.613	3.2840	1	10	No
Tepotinib [59]		492.6	4.0079	0	8	Yes
Topotecan [60]		421.45	1.8468	2	8	Yes
Trametinib [61]		615.4	3.9401	2	8	No
Trilaciclib [62]		546.559	2.7245	2	8	No

of molecular dynamics simulation.

2. Methodology

2.1. Docking of FDA approved anti-lung cancer drugs with Mpro, PLpro and Spike proteins of SARS-CoV-2

a. Ligand and protein preparation

The crystal structure of SARS-CoV-2 main-protease (Mpro; PDB ID:6LU7), papain like-protease (PLpro; PDB ID:6W9C) and spike glycoprotein protein (PDB ID:6VXX) were retrieved from Protein Data-bank (www.rcsb.org). The “sdf” files (3D-conformer) of anti-lung cancer drugs were downloaded from PubChem (<https://pubchem.ncbi.nlm.nih.gov/>) and was converted to respective pdb files. All the structures of proteins were cleaned by removing hetero-atoms and water molecules using UCSF Chimera [30].

b. Docking

Autodock Vina [31] was used to evaluate the best binding sites of the drugs against Mpro, PLpro and spike protein. To elucidate the binding site identification along with structural features of protein-drug composite UCSF Chimera [30] and Discovery Studio Visualizer [32] have been used.

2.2. ADMET properties evaluation

pKCSM [33] (<http://biosig.unimelb.edu.au/pkcsml/prediction>) online tool was used to elucidate the ADMET profiling of these drugs.

2.3. Molecular dynamics (MD) simulation studies

Molecular dynamics simulation for a period of 10ns were performed with energy minimized CAP docked Mpro, PLpro and Spike protein using Gromacs 5.1 [34] package. The TIP3P solvation model [35] implemented on CHARMM36-mar2019 force field [36] were used during MD-simulation. Required input parameters for the drug (CAP) were created with the help of CGenFF-server. To make the system electrically neutral adequate number of ions were added within a cubical box having length of 10 Å. 100ps NVT equilibration were performed with the energy minimized conformation followed by 100ps NPT equilibration with 2fs time steps. A cut-off of 1.0 nm for both electrostatic and Van der Waals were set for the above equilibration process. By applying smooth particle mesh Ewald (PME) method long range interactions were measured [37]. With the similar electrostatic and Van der Waals cut-off the MD-simulations were performed for 10ns. A modified Berendsen thermostat and a Parinello-Rahman barostat were used with reference temperature and pressure at 300 K and 1 bar respectively.

2.4. Binding free energy calculation

With the use of the following equations, the Poisson-Boltzmann surface area (MM-PBSA) method [38] (based on the Gromacs tool g_mmpbsa package) was used to compute the binding free energies of the supplied protein-ligand complexes.

$$\Delta G_{\text{bind}} = G_{\text{w-complex}} - G_{\text{w-protein}} - G_{\text{w-drug}} \quad (1)$$

$$G_{\text{w-complex}} = \langle E_{\text{MM}} \rangle + \langle G_{\text{sol}} \rangle - \text{TS} \quad (2)$$

$$E_{\text{MM}} = E_{\text{bonded}} + E_{\text{non-bonded}} = E_{\text{bonded}} + (E_{\text{vdW}} + E_{\text{elec}}) \quad (3)$$

$$G_{\text{sol}} = G_{\text{polar}} + G_{\text{non-polar}} = G_{\text{polar}} + (\gamma \text{SASA} + b) \quad (4)$$

Where, $G_{\text{w-complex}}$ is the total free energy of the protein and drug complex, $G_{\text{w-protein}}$, $G_{\text{w-drug}}$ are the free energies of the protein and drug

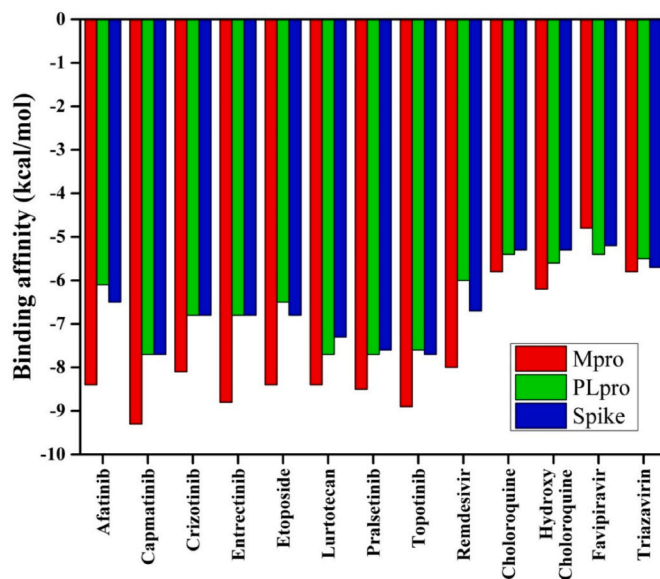


Fig. 1. Docking score of anti-lung cancer drugs and comparison with Remdesivir, Chloroquine, Hydroxychloroquine, Favipiravir, Triazavirin against Mpro, PLpro and Spike proteins.

Table 2

Inhibition constant (K_i) of anti-lung cancer drugs with Mpro, PLpro and spike protein of SARS-CoV-2.

Name of the anti -lung cancer drugs and Drugs	$K_i(\mu\text{M})$		
	Mpro	PLpro	Spike protein
Afatinib	0.71	34.23	17.44
Capmatinib	0.15	2.31	2.31
Crizitinib	1.17	10.52	10.52
Entrectinib	0.36	10.52	10.52
Etoposide	0.71	17.44	10.52
Lurilotecan	0.71	2.31	4.53
Pralsetinib	0.59	2.31	2.73
Topotinib	0.31	2.73	2.31
Remdesivir	1.39	40.51	12.45
Chloroquine	56.76	111.39	131.84
Hydroxychloroquine	28.92	79.51	131.84
Favipiravir	306.26	111.39	156.05
Triazavirin	56.76	94.11	67.18

respectively. E_{MM} is the average MM potential energy including bonding, non-bonding energies, G_{sol} is the free energy of solvation including polar and non-polar energies. SASA is the solvent accessible surface area, γ is the coefficient of surface tension of solvent and b is the fitting parameter. TS is not considered by g_mmpbsa.

3. Results and discussion

The structure, molecular weight, partition co-efficient (log P) and number of H-bonds donor-acceptor sites of anti-lung cancer drugs and the drugs that follows the Lipinski's rule [27] are tabulated in Table 1. Among the 24 selected anti-lung cancer drugs, 17 drugs follow the Lipinski's rule that means all these 17 drugs do not have more than 5 hydrogen bond donors and 10 hydrogen bond acceptors and their molecular weight less than 500 Da with partition coefficient is less than 5.

Based on drug-likeness properties, 17 anti-lung cancer drugs were virtually screened against SARS-CoV-2 Mpro, PLpro and spike proteins.

3.1. Molecular docking

The binding affinity of 17 drugs were tabulated in Table S1 which

Table 3
Toxicity prediction of anti-lung cancer drug.

Drugs	AMES toxicity	Max. tolerated dose (human)	hERG I inhibitor	hERG II inhibitor	Oral Rat Acute Toxicity (LD50) (mol/kg)	Oral Rat Chronic Toxicity (LOAEL) (log mg/kg_bw/day)	Hepatotoxicity	Skin Sensitisation	T.Pyiformis toxicity (log ug/L)	Minnow toxicity (log mM)
Afatinib	No	-0.097	No	Yes	2.62	1.09	Yes	No	0.302	3.416
Capmatinib	No	0.371	No	Yes	2.60	0.77	Yes	No	0.285	0.785
Crizotinib	No	-0.095	No	Yes	3.52	1.57	Yes	No	0.296	0.942
Entrectinib	No	0.443	No	Yes	2.38	1.68	Yes	No	0.285	2.884
Etoposide	No	0.171	No	No	3.25	2.43	No	No	0.285	2.217
Lurtotecan	No	0.171	No	Yes	2.69	2.24	Yes	No	0.285	0.734
Pralsetinib	No	0.496	No	Yes	2.61	1.83	Yes	No	0.285	0.939
Tepotinib	No	0.828	No	Yes	2.77	0.95	Yes	No	0.285	-1.164

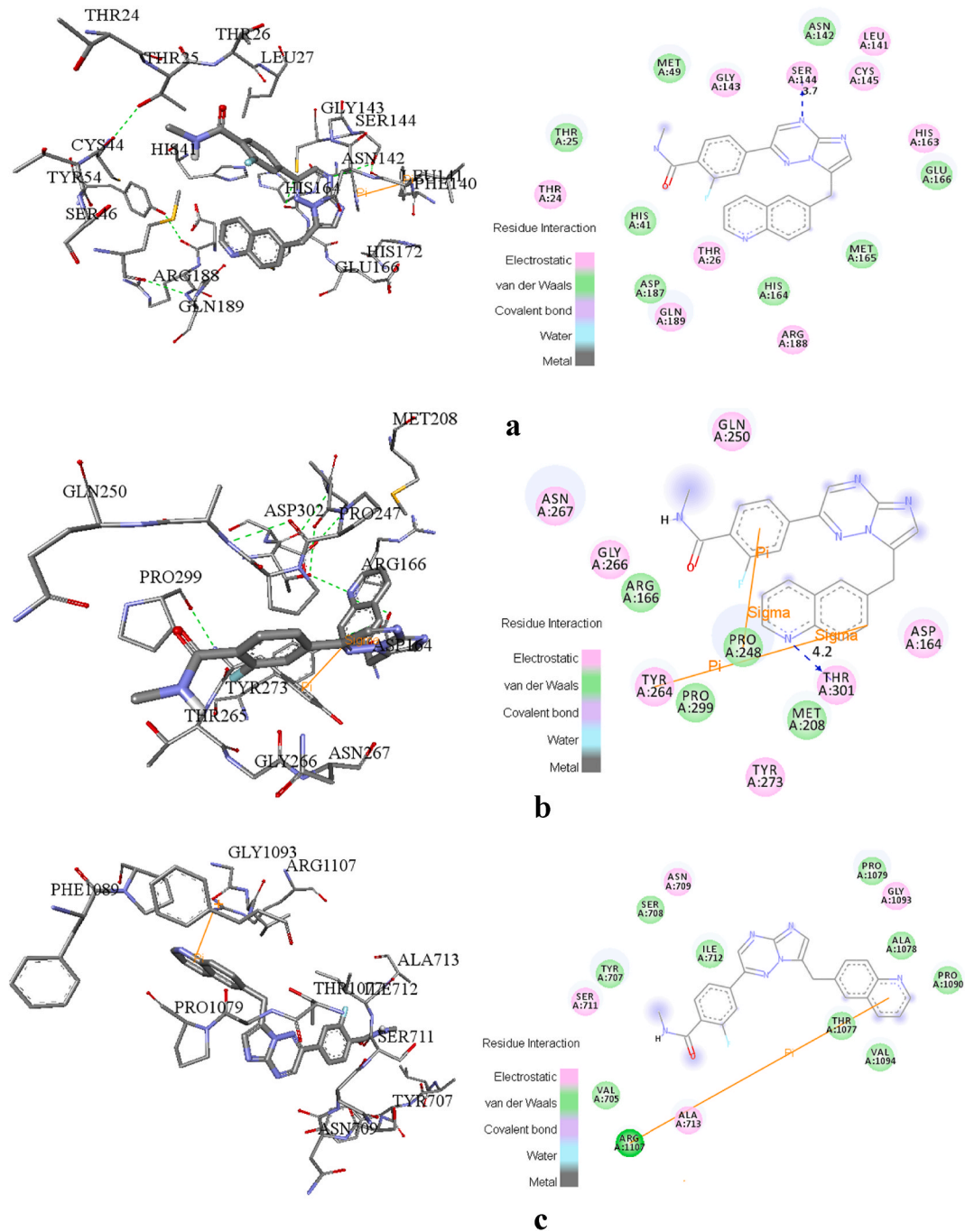


Fig. 2. Binding interactions of CAP with (a) Mpro; (b) PLpro; (c) Spike protein of SARS-CoV-2.

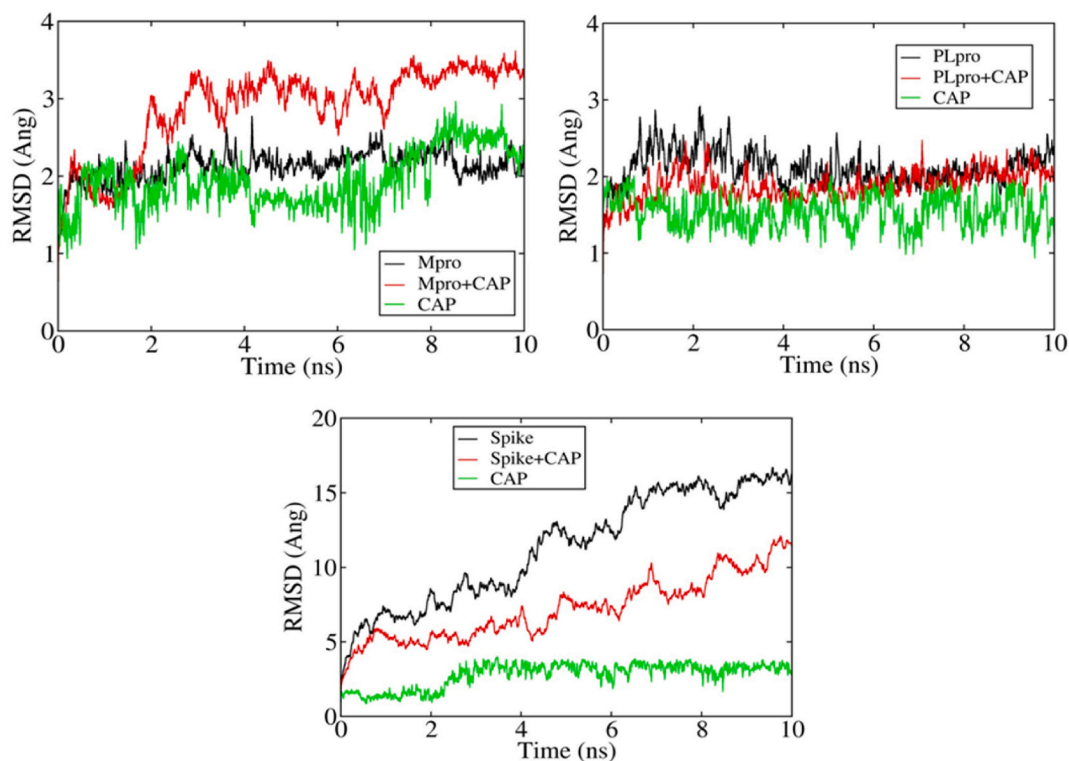


Fig. 3. RMSD plots for docked and undocked Mpro, PLpro and Spike Protein.

revealed that 8 drugs have higher binding affinity compared to well-known drugs like remdesivir, chloroquine, hydroxychloroquine, favipiravir, trizavirin as shown in Fig. 1. Highest binding affinity was experienced by Capmatinib (CAP) against Mpro (-9.3 kcal/mol), PLpro (-7.7 kcal/mol), Spike (-7.7 kcal/mol) of SARS-CoV-2.

Inhibition constant (K_i) value is another important indicator of

binding between the drug and the protein. Smaller value of K_i implies strong binding affinity [63]. In our study, lowest K_i value (0.15) was shown by CAP against Mpro, a reflection of its highest activity against this protein. Table 2 showed that CAP has lowest K_i values against the three proteins (Mpro, PLpro, Spike) which revealed that it was the most active drug against SARS-CoV-2 in comparison to other selected drugs.

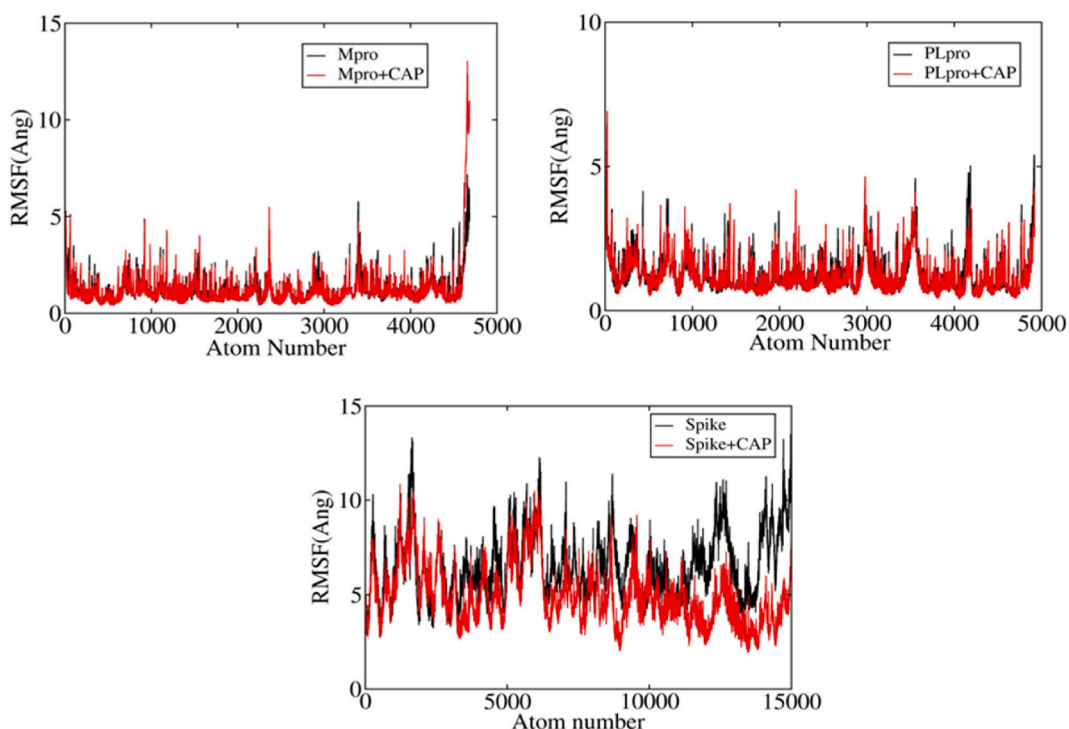


Fig. 4. RMSF plots for docked and undocked (a) Mpro, (b) PLpro and (c) Spike Protein.

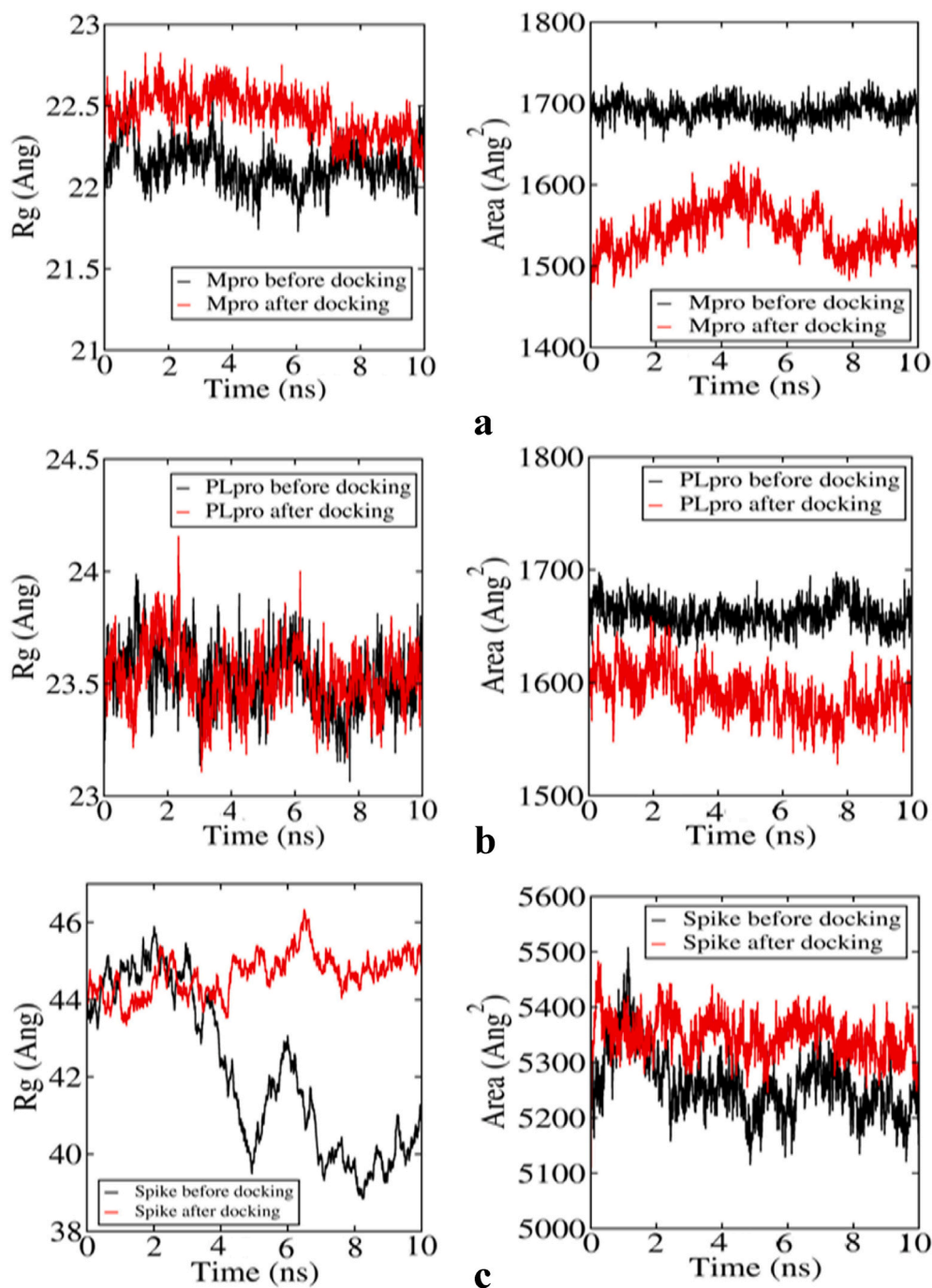


Fig. 5. Radius of gyration (left) and SASA (right) plots for Mpro, PLpro and Spike protein.

3.2. ADMET analysis

Moreover, for the determination of level of toxicity of these 8 selected drugs, we have analysed ADME [64] profile by pkCSM online server. ADME studies are also very important to determine the pharmacodynamic parameters of the selected drugs. According to the study of pharmacokinetic properties, all drugs were effectively absorbed by the gastro-intestinal part with low blood brain-barrier (BBB) permeability value which is shown in Table S2. Toxicity studies are very useful for the compounds to determine the tolerability towards human body. All the selected drugs have negative AMES toxicity, indicates they were not carcinogenic or mutagenic. All drugs have negative hERG1 inhibition activity. The LD50 values of the 8 drugs fall in between 2.6 and 3.5 (mol/kg) while the chronic oral rat toxicity (LOAEL) values vary in

between 0.5 and 2.4 (log mg/kg_{bw}/day). None of the drugs showed skin sensitisation. Hepatotoxicity, T.pyriformins and minnow toxicity values are also available in Table 3.

The binding interactions between CAP and target proteins viz. Mpro, PLpro and spike protein of SARS-CoV-2 are illustrated in Fig. 2. Major interactions that are responsible for binding are H-bonding, electrostatic and Van der Waals interactions. CAP showed H-bonding interactions with SER144 amino acid of Mpro (Fig. 2a), THR301 of PLpro (Fig. 2b); electrostatic interaction with amino acid residues GLY143, SER144, LEU141, CYS145, HIS163, THR26, THR24, ARG188, GLN189 of Mpro, GLN250, ASP164, THR301, TYR264, TYR273, GLY266, ASN267 of PLpro and ASN709, GLY1093, SER711, ALA713 of spike protein (Fig. 2c).

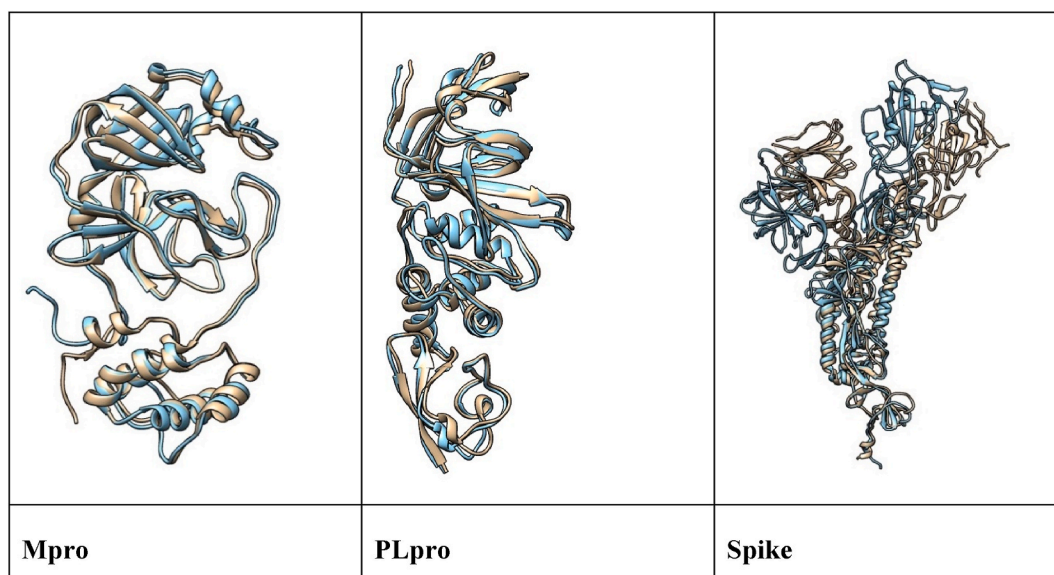


Fig. 6. Conformational changes of undocked and docked proteins at 10ns.

3.3. MD Simulation

Root mean square deviation value is an indicator of the stability of the protein-ligand complex [65]. RMSD was calculated considering the proteins (Mpro, PLpro, Spike) backbone with respect to their initial conformations. As depicted in Fig. 3, RMSD of Mpro-CAP remains stable up-to 2 ns. After 2 ns RMSD value of Mpro-CAP increased from 2 Å

whereas RMSD value of PLpro-CAP showed a balanced system after 2 ns. RMSD of Spike-CAP is more stable than spike protein only throughout the run.

Root mean square fluctuation analysis is another essential parameter for identifying the rigid and flexible regions for the binding pocket of the protein. It is a standard measure of the deviation of the atoms from its original position. Furthermore, it can be used to assess the flexibility of

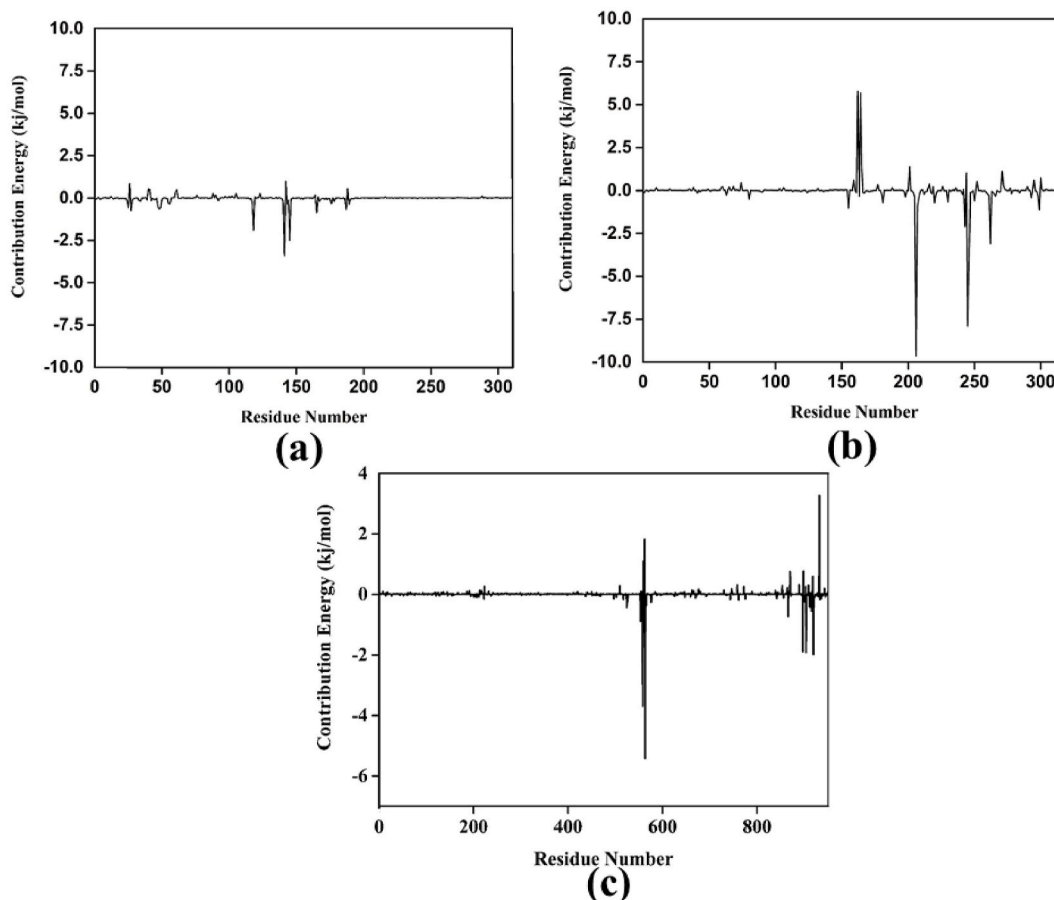


Fig. 7. Contribution Energy plots for docked (a) Mpro,(b) PLpro and (c) Spike Protein.

Table 4
Different types of interaction energies between proteins of SARS-CoV-2 and CAP.

Protein-CAP complex	Van der Waals energy (kJ/mol)	Electrostatic energy (kJ/mol)	Polar solvation energy (kJ/mol)	SASA energy (kJ/mol)	Binding energy (kJ/mol)
Mpro-CAP	-69.613	-11.267	54.736	-5.542	-31.691
PLpro-CAP	-104.764	-10.372	88.404	-8.151	-34.883
Spike-CAP	-82.160	-33.701	97.081	2.884	-15.897

the backbone atoms of the protein structure as well as the ligand [66]. A thorough study of the RMSF curves of the free proteins (Mpro, PLpro, Spike) and their complexes showed RMSF fluctuations of all amino acids located in the active site of the proteins. Lowest fluctuation was observed for PLpro-CAP. Fig. 4 revealed that, the fluctuations of residues for the docked structures of Mpro and spike protein are quite low with respect to their undocked one.

The radius of gyration (Rg) is a constructive tool for a clear understanding of folding properties and compactness of the protein and protein-ligand complexes. The influence of drug molecule in a protein structure can be demonstrated from the conformational changes of Rg. Higher the Rg value of a protein molecule specifies its loose packing, while, lower Rg value specifies tight packing of the protein structure. For PLpro, before and after docking compactness did not deviate much. In case of Mpro and spike protein, the Rg value of docked protein changes after 7ns and 4ns respectively. The Rg plot is shown in Fig. 5 (left column). Solvent-accessible surface area (SASA) values of the simulated complexes were analysed to evaluate the changes in protein surface exposure to the solvents. Higher SASA values indicate the expansion of the surface area, whereas lower SASA values indicate the compression of the protein volume. Docked Mpro and PLpro have the lower SASA values than their corresponding undocked structures whereas docked structure of spike protein had the higher value than its corresponding undocked one. Fig. 5 (right column) reflected that protein surface area decreased after docking for Mpro and PLpro.

To evaluate the conformational changes of the protein molecules, we have taken the snapshots at each 1ns during the MD-simulation. All the conformational changes during the progression of MD are represented in Fig. S1. The significant conformational changes are observed at 8–9ns and 6–7ns for Mpro and PLpro respectively. Major change of conformation is involved in case of the spike protein. All these results are in concordance with the RMSD and RMSF plots. Fig. 6 represents conformational changes before and after docking of proteins with CAP at 10ns.

Furthermore, to support the conformational alternation of the amino acid residues in protein, we have studied the sequence analysis of the proteins (Mpro, PLpro and Spike) before and after docking represented in Fig. S2. In case of Mpro, the change of the amino acids residue numbers involved from 1 to 4, 52 & 54 and 306 to 311 whereas in PLpro, the changes involved 1 to 2, 225 to 226, 229 to 230 and 318 to 319. A drastic change occurs in the case of spike protein due to interaction of the CAP. The change of the amino acid residue in spike protein involved from 1 to 1060. All the results are finally supported by Fig. 7 that represents contribution energy with respect to residue number.

3.4. MMPBSA binding energy analysis

To calculate the interaction between proteins of SARS-CoV-2 and CAP we have performed MMPBSA binding energy calculation as shown in Table 4. The negative binding energy values suggests stabilisation of protein-ligand complexes [38]. The positive value of polar solvation energy indicates that little contribution to the ligand binding with protein.

4. Conclusion

In our present study, we have carried out a systematic analysis of inhibitory efficacy of 8 anti-lung cancer drugs in comparison with some well-known drugs viz. Remdesivir, Chloroquine, Hydroxychloroquine, Favipiravir, Triazavirin against Mpro, PLpro and spike proteins of SARS-CoV-2. CAP showed highest binding affinity and lowest K_i values against these proteins. ADMET profiling suggests that CAP has lower toxicity level. Furthermore, MD simulation followed by the analysis of RMSD, RMSF, Gyrate and SASA plots explain the significant binding of CAP with the selected proteins. GMPBSA calculation revealed that CAP has highest binding energy with PLpro with respect to other selected proteins. As per our study, CAP can show substantial inhibitory efficiency against these selected proteins of SARS-CoV-2. Hope, these findings provide paves a new way to discover potential drug to combat COVID-19.

CRedit authorship contribution statement

Rahimasoom Reza: Writing – original draft, Data curation. **Tanmoy Dutta:** Methodology. **Nabajyoti Baildya:** Investigation. **Narendra Nath Ghosh:** Software. **Abdul Ashik Khan:** Data curation, Conceptualization. **Rajesh Kumar Das:** Supervision, Writing – review & editing.

Declaration of competing interest

The authors declare no conflicting interest in the present work.

Data availability

Data is available upon request to the corresponding author.

Appendix A. Supplementary data

Supplementary data to this article can be found online at <https://doi.org/10.1016/j.micpath.2022.105615>.

References

- [1] X. Xu, P. Chen, J. Wang, J. Feng, H. Zhou, X. Li, et al., Evolution of the novel coronavirus from the ongoing Wuhan outbreak and modeling of its spike protein for risk of human transmission, *Science China Life Sciences* 63 (2020) 457–460.
- [2] N. Zhu, D. Zhang, W. Wang, X. Li, B. Yang, J. Song, et al., A novel coronavirus from patients with pneumonia in China, 2019, *New England journal of medicine* 8 (2020) 727–733.
- [3] P. Zhou, X.-L. Yang, X.-G. Wang, B. Hu, L. Zhang, W. Zhang, et al., A pneumonia outbreak associated with a new coronavirus of probable bat origin, *nature* 579 (2020) 270–273.
- [4] T. Acter, N. Uddin, J. Das, A. Akhter, T.R. Choudhury, S. Kim, Evolution of severe acute respiratory syndrome coronavirus 2 (SARS-CoV-2) as coronavirus disease 2019 (COVID-19) pandemic: a global health emergency, *Science of the Total Environment* 730 (2020), 138996.
- [5] A.A. Khan, T. Dutta, M. Palas Mondal, S.K.C. Mandal, M. Ahmed, N. Baildya, et al., Novel Coronavirus Disease (COVID-19): an extensive study on evolution, global health, drug targets and vaccines, 2021, *Int J Clin Virol* (2021) 54–69.
- [6] L.E. Gralinski, V.D. Menachery, Return of the coronavirus: 2019-nCoV, *Viruses* 12 (2020) 135.
- [7] R. Verity, L.C. Okell, I. Dorigatti, P. Winskill, C. Whittaker, N. Imai, et al., Estimates of the severity of coronavirus disease 2019: a model-based analysis, *The Lancet infectious diseases* 20 (2020) 669–677.
- [8] H. Wang, Z. Wang, Y. Dong, R. Chang, C. Xu, X. Yu, et al., Phase-adjusted estimation of the number of coronavirus disease 2019 cases in Wuhan, China, *Cell discovery* 6 (2020) 1–8.
- [9] T. Chorba, The concept of the crown and its potential role in the downfall of coronavirus, *Emerging Infectious Diseases* 26 (2020) 2302.
- [10] K. EL Azhari, K. Miyara, A. Saadia, S. Souat, A. Badou, *Emerging COVID-19 vaccines: safety, efficacy and universality*, *Moroccan Journal of Public Health* 2 (2021) 89–105.
- [11] J.C. Ferreira, W.M. Rabeih, Biochemical and biophysical characterization of the main protease, 3-chymotrypsin-like protease (3CLpro) from the novel coronavirus SARS-CoV 2, *Scientific reports* 10 (2020) 1–10.
- [12] Y.M. Báez-Santos, S.E.S. John, A.D. Mesecar, The SARS-coronavirus papain-like protease: structure, function and inhibition by designed antiviral compounds, *Antiviral research* 115 (2015) 21–38.

- [13] H.B. Gelberg, Alimentary system and the peritoneum, omentum, mesentery, and peritoneal cavity, *Pathologic basis of veterinary disease* (2017) 324.
- [14] Z.T. Muhseen, A.R. Hameed, H.M. Al-Hasani, M.T. ul Qamar, G. Li, Promising terpenes as SARS-CoV-2 spike receptor-binding domain (RBD) attachment inhibitors to the human ACE2 receptor: integrated computational approach, *Journal of molecular liquids* 320 (2020), 114493.
- [15] A. Rabaan, S. Al-Ahmed, R. Sah, R. Tiwari, M. Yattoo, S. Patel, et al., SARS-CoV-2/COVID-19 and Advances in Developing Potential Therapeutics and Vaccines to Counter This Emerging Pandemic Virus—A Review, Preprints, 2020, 2020040075, 1020944/preprints202004.75.v1.
- [16] J.A. Al-Tawfiq, A.H. Al-Homoud, Z.A. Memish, Remdesivir as a possible therapeutic option for the COVID-19, *Travel medicine and infectious disease* 34 (2020), 101615.
- [17] N. Baildya, N.N. Ghosh, A.P. Chattopadhyay, Inhibitory capacity of Chloroquine against SARS-COV-2 by effective binding with Angiotensin converting enzyme-2 receptor: an insight from molecular docking and MD-simulation studies, *Journal of Molecular Structure* 1230 (2021), 129891.
- [18] N. Baildya, N.N. Ghosh, A.P. Chattopadhyay, Inhibitory activity of hydroxychloroquine on COVID-19 main protease: an insight from MD-simulation studies, *Journal of Molecular Structure* 1219 (2020), 128595.
- [19] A. Roy, R. Das, D. Roy, S. Saha, N.N. Ghosh, S. Bhattacharyya, et al., Encapsulated hydroxychloroquine and chloroquine into cyclic oligosaccharides are the potential therapeutics for COVID-19: insights from first-principles calculations, *Journal of molecular structure* (2021), 131371.
- [20] K. Naydenova, K.W. Muir, L.-F. Wu, Z. Zhang, F. Coscia, M.J. Peet, et al., Structure of the SARS-CoV-2 RNA-dependent RNA polymerase in the presence of favipiravir-RTP, *Proceedings of the National Academy of Sciences* (2021) 118.
- [21] X. Wu, K. Yu, Y. Wang, W. Xu, H. Ma, Y. Hou, et al., The efficacy and safety of Triazavirin for COVID-19: a trial protocol, *Engineering* 6 (2020) 1199–1204.
- [22] T.M. Abd El-Aziz, J.D. Stockand, Recent progress and challenges in drug development against COVID-19 coronavirus (SARS-CoV-2)—an update on the status, *Infection, Genetics and Evolution* 83 (2020), 104327.
- [23] M. Mandal, S.K. Chowdhury, A.A. Khan, N. Baildya, T. Dutta, D. Misra, et al., Inhibitory efficacy of RNA virus drugs against SARS-CoV-2 proteins: an extensive study, *Journal of molecular structure* 1234 (2021), 130152.
- [24] N. Baildya, A.A. Khan, N.N. Ghosh, T. Dutta, A.P. Chattopadhyay, Screening of potential drug from Azadirachta Indica (Neem) extracts for SARS-CoV-2: an insight from molecular docking and MD-simulation studies, *Journal of molecular structure* 1227 (2021), 129390.
- [25] T. Dutta, N. Baildya, A.A. Khan, N.N. Ghosh, Inhibitory effect of anti-HIV compounds extracted from Indian medicinal plants to retard the replication and transcription process of SARS-CoV-2: an insight from molecular docking and MD-simulation studies, *Network Modeling Analysis in Health Informatics and Bioinformatics* 10 (2021) 1–11.
- [26] T. Dutta, S. Ghorai, A.A. Khan, N. Baildya, N.N. Ghosh, Screening of potential anti-HIV compounds from *Achyranthes aspera* extracts for SARS-CoV-2: an insight from molecular docking study, *Journal of Physics: Conference Series* (2021), 012042. IOP Publishing.
- [27] M.-Q. Zhang, B. Wilkinson, Drug discovery beyond the ‘rule-of-five’, *Current opinion in biotechnology* 18 (2007) 478–488.
- [28] A.A. Khan, N. Baildya, T. Dutta, N.N. Ghosh, Inhibitory efficiency of potential drugs against SARS-CoV-2 by blocking human angiotensin converting enzyme-2: Virtual screening and molecular dynamics study, *Microbial Pathogenesis* 152 (2021), 104762.
- [29] U. Norinder, C.A. Bergström, Prediction of ADMET properties, *ChemMedChem: Chemistry Enabling Drug Discovery* 1 (2006) 920–937.
- [30] E.F. Pettersen, T.D. Goddard, C.C. Huang, G.S. Couch, D.M. Greenblatt, E.C. Meng, et al., UCSF Chimera—a visualization system for exploratory research and analysis, *Journal of computational chemistry* 25 (2004) 1605–1612.
- [31] R. Huey, G.M. Morris, S. Forli, Using AutoDock 4 and AutoDock Vina with AutoDockTools: a Tutorial, vol. 10550, The Scripps Research Institute Molecular Graphics Laboratory, 2012, 92037.
- [32] D.S. Biovia, Discovery Studio Modeling Environment, 2017. Release.
- [33] D.E. Pires, T.L. Blundell, D.B. Ascher, pkCSM: predicting small-molecule pharmacokinetic and toxicity properties using graph-based signatures, *Journal of medicinal chemistry* 58 (2015) 4066–4072.
- [34] H.J. Berendsen, D. van der Spoel, R. van Drunen, GROMACS: a message-passing parallel molecular dynamics implementation, *Computer physics communications* 91 (1995) 43–56.
- [35] S. Lee, A. Tran, M. Allsopp, J.B. Lim, J. Hénin, J.B. Klauda, CHARMM36 united atom chain model for lipids and surfactants, *The journal of physical chemistry B* 118 (2014) 547–556.
- [36] S. Boonstra, P.R. Onck, E. van der Giessen, CHARMM TIP3P water model suppresses peptide folding by solvating the unfolded state, *The journal of physical chemistry B* 120 (2016) 3692–3698.
- [37] M. Harvey, G. De Fabritiis, An implementation of the smooth particle mesh Ewald method on GPU hardware, *Journal of chemical theory and computation* 5 (2009) 2371–2377.
- [38] R. Kumari, R. Kumar, O.S.D.D. Consortium, A. Lynn, g_mmpbsa: A GROMACS tool for high-throughput MM-PBSA calculations, *Journal of chemical information and modeling* 54 (2014) 1951–1962.
- [39] R.T. Dunto, G.M. Keating, Afatinib: first global approval, *Drugs* 73 (2013) 1503–1515.
- [40] S. Peters, D.R. Camidge, A.T. Shaw, S. Gadgeel, J.S. Ahn, D.-W. Kim, et al., Alectinib versus crizotinib in untreated ALK-positive non-small-cell lung cancer, *New England Journal of Medicine* 377 (2017) 829–838.
- [41] D.R. Camidge, H.R. Kim, M.-J. Ahn, J.C.-H. Yang, J.-Y. Han, J.-S. Lee, et al., Brigatinib versus crizotinib in ALK-positive non-small-cell lung cancer, *New England Journal of Medicine* 379 (2018) 2027–2039.
- [42] C.J. Thomas, N.J. Rahier, S.M. Hecht, Camptothecin: current perspectives, *Bioorganic & medicinal chemistry* 12 (2004) 1585–1604.
- [43] J.F. Vansteenkiste, C. Van De Kerkhove, E. Wauters, P. Van Mol, Capmatinib for the treatment of non-small cell lung cancer, *Expert review of anticancer therapy* 19 (2019) 659–671.
- [44] A.T. Shaw, D.-W. Kim, R. Mehra, D.S. Tan, E. Felip, L.Q. Chow, et al., Ceritinib in ALK-rearranged non-small-cell lung cancer, *N Engl j med* 370 (2014) 1189–1197.
- [45] A.T. Shaw, U. Yasothan, P. Kirkpatrick, Crizotinib. *Nature Reviews Drug Discovery* 10 (2011).
- [46] Y.-L. Wu, Y. Cheng, X. Zhou, K.H. Lee, K. Nakagawa, S. Niho, et al., Dacomitinib versus gefitinib as first-line treatment for patients with EGFR-mutation-positive non-small-cell lung cancer (ARCHER 1050): a randomised, open-label, phase 3 trial, *The Lancet Oncology* 18 (2017) 1454–1466.
- [47] M.P. Garrido, I. Torres, M. Vega, C. Romero, Angiogenesis in gynecological cancers: role of neurotrophins, *Frontiers in oncology* 9 (2019) 913.
- [48] J.M. Henwood, R.N. Brogden, Etoposide. *Drugs*. 39 (1990) 438–490.
- [49] J. Dowell, J.D. Minna, P. Kirkpatrick, Erlotinib hydrochloride, *Nature Reviews Drug Discovery* 4 (2005).
- [50] D. Brehmer, Z. Greff, K. Godl, S. Blencke, A. Kurtenbach, M. Weber, et al., Cellular targets of gefitinib, *Cancer research* 65 (2005) 379–382.
- [51] S. Noble, K.L. Goa, Gemcitabine. *Drugs*. 54 (1997) 447–472.
- [52] B.J. Solomon, B. Besse, T.M. Bauer, E. Felip, R.A. Soo, D.R. Camidge, et al., Lorlatinib in patients with ALK-positive non-small-cell lung cancer: results from a global phase 2 study, *The Lancet Oncology* 19 (2018) 1654–1667.
- [53] K.T. Flaherty, J.P. Stevenson, C.J. Twelves, P.J. O’Dwyer, *The Clinical Development of Lurtotecan*. Camptothecins in Cancer Therapy, Springer, 2005, pp. 301–316.
- [54] E.C. Vonderheid, E.T. Tan, A.F. Kantor, L. Shrager, B. Micaly, E.J. Van Scott, Long-term efficacy, curative potential, and carcinogenicity of topical mechlorethamine chemotherapy in cutaneous T cell lymphoma, *Journal of the American Academy of Dermatology* 20 (1989) 416–428.
- [55] J.-C. Soria, Y. Ohe, J. Vansteenkiste, T. Reungwetwattana, B. Chewaskulyong, K. H. Lee, et al., Osimertinib in untreated EGFR-mutated advanced non-small-cell lung cancer, *New England journal of medicine* 378 (2018) 113–125.
- [56] N. Hanna, F.A. Shepherd, F.V. Fossella, J.R. Pereira, F. De Marinis, J. Von Pawel, et al., Randomized phase III trial of pemetrexed versus docetaxel in patients with non-small-cell lung cancer previously treated with chemotherapy, *Journal of clinical oncology* 22 (2004) 1589–1597.
- [57] D. Lee, V. Subbiah, J. Gainor, M. Taylor, V. Zhu, R. Doebele, et al., Treatment with pralsetinib (formerly BLU-667), a potent and selective RET inhibitor, provides rapid clearance of ctDNA in patients with RET-altered non-small cell lung cancer (NSCLC) and medullary thyroid cancer (MTC), *Annals of Oncology* 30 (2019) ix122.
- [58] A. Drilon, G.R. Oxnard, D.S. Tan, H.H. Loong, M. Johnson, J. Gainor, et al., Efficacy of selpercatinib in RET fusion-positive non-small-cell lung cancer, *New England Journal of Medicine* 383 (2020) 813–824.
- [59] P.K. Paik, E. Felip, R. Veillon, H. Sakai, A.B. Cortot, M.C. Garassino, et al., Tepotinib in non-small-cell lung cancer with MET exon 14 skipping mutations, *New England Journal of Medicine* 383 (2020) 931–943.
- [60] J. Von Pawel, J.H. Schiller, F.A. Shepherd, S.Z. Fields, J. Kleisbauer, N.G. Chrysson, et al., Topotecan versus cyclophosphamide, doxorubicin, and vincristine for the treatment of recurrent small-cell lung cancer, *Journal of Clinical Oncology* 17 (1999) 658.
- [61] D. Planchard, B. Besse, H.J. Groen, P.-J. Souquet, E. Quoix, C.S. Baik, et al., Dabrafenib plus trametinib in patients with previously treated BRAFV600E-mutant metastatic non-small cell lung cancer: an open-label, multicentre phase 2 trial, *The Lancet Oncology* 17 (2016) 984–993.
- [62] L.L. Hart, R. Ferrarotto, Z.G. Andric, J.T. Beck, J. Subramanian, D.Z. Radosavljevic, et al., Myelopreservation with trilaciclib in patients receiving topotecan for small cell lung cancer: results from a randomized, double-blind, placebo-controlled phase II study, *Advances in therapy* 38 (2021) 350–365.
- [63] D. Compton, K.C. Rice, B.R. De Costa, R. Razdan, L.S. Melvin, M.R. Johnson, et al., Cannabinoid structure-activity relationships: correlation of receptor binding and in vivo activities, *Journal of Pharmacology and Experimental Therapeutics* 265 (1993) 218–226.
- [64] S. Ekins, C.L. Waller, P.W. Swaan, G. Cruciani, S.A. Wrighton, J.H. Wikel, Progress in predicting human ADME parameters in silico, *Journal of pharmacological and toxicological methods* 44 (2000) 251–272.
- [65] C. Guilbert, T.L. James, Docking to RNA via root-mean-square-deviation-driven energy minimization with flexible ligands and flexible targets, *Journal of chemical information and modeling* 48 (2008) 1257–1268.
- [66] S. Mathpal, T. Joshi, P. Sharma, T. Joshi, H. Pundir, V. Pande, et al., A dynamic simulation study of FDA drug from zinc database against COVID-19 main protease receptor, *Journal of Biomolecular Structure and Dynamics* (2020) 1–17.